using the TMB substrate kit (Pierce). Again, between each step, the plates were washed three times with PBS.

Passive transfer of human IgG to mice. Passive IgG transfer to mice was conducted as described elsewhere[24]. Six-week-old female C57BL/6J mice were intraperitoneally injected with 40 mg IgG of Ct. 2 and Pt. 2 every day for 15 days. IgG was sterilized with a 0.22-μm filter (Millipore) and dissolved in 400 μl PBS. The mice were sacrificed on day 16 under deep anesthesia. We intraperitoneally injected 300 mg/kg of cyclophosphamide monohydrate (10 mg/ml in 0.9% NaCl) at 24 hrs after the first IgG injection to suppress any active immune response to the human protein[25]. We also injected IgG of Pt. 2 to two additional mice to confirm consistency, and we analyzed a representative mouse in detail. The passive IgG transfer studies were approved by the Animal Care and Use Committee of the Nagoya University.

We detected AChR by Alexa594-labeled α-bungarotoxin (Molecular Probes), ColQ by 1:100 of anti-ColQ antibody described above, and MuSK by 1:100 of anti-MuSK antibody (C-19, Santa Cruz). Signals were quantified by the BZ-9000 microscope (Keyence) equipped with the Dynamic Cell Count software BZ-H1C (Keyence).

Results

MuSK-IgG recognizes NMJ of a muscle section of *Colq-/-* mouse. We first confirmed that human MuSK-IgG recognizes the mouse NMJ. We isolated IgG from serum of MuSK-MG patients and confirmed the purity of IgG by Coomassie staining of nonreducing (figure 1A) and reducing (figure 1B) SDS-PAGEs. We then overlaid MuSK-IgG on quadriceps muscle sections of *Colq*-/- mice[22]. IgG of Ct. 1 was not bound to the NMJ, whereas IgGs of Pts. 1 and 2 colocalized to the NMJs (figure 1C). Human MuSK-IgG thus has the potential to bind to the mouse NMJ.

***In vitro* overlay assay discloses that MuSK-IgG blocks binding of ColQ-tailed AChE to the NMJ of a muscle section of *Colq-/-* mouse.** We previously demonstrated that the purified recombinant human ColQ-tailed AChE protein complex could bind to sections of the frog NMJs[23] and the mouse NMJs (in preparation) *in vitro*. Using the *in vitro* overlay assay, we next examined whether MuSK-IgG blocks anchoring of ColQ-tailed AChE to the mouse NMJs. We incubated a muscle section of *Colq*-/- mice with MuSK-IgG overnight at 4 °C and overlaid human ColQ-tailed AChE followed by histological visualization of ColQ and AChR (figure 2). In the presence of IgG of Ct. 1, ColQ was colocalized with AChRs, whereas, in the presence of four MuSK-IgGs, no ColQ-signal was observed at the NMJs.

***In vitro* plate-binding assay shows that MuSK-IgG blocks binding of ColQ-tailed AChE**

but not of LRP4 to MuSK. We next quantified an effect of MuSK-IgG on an interaction of human ColQ and human MuSK by an *in vitro* plate-binding assay. We synthesized and purified the myc-tagged extracellular domain of human MuSK (hMuSKect-myc). We then incubated an hMuSKect-coated plate with variable concentrations of control IgG or MuSK-IgG, and added a fixed amount of the purified recombinant human ColQ-tailed AChE. In two controls, AChE remained bound even in the presence of 100 μg of IgG, whereas in four MuSK-MG patients the numbers of bound AChE were proportionally decreased with increasing amounts of the patient's IgG (figure 3A).

We also quantified an effect of MuSK-IgG on an interaction of the extracellular domains of MuSK and LRP4. IgG of neither Ct. 2 nor Pt. 2 blocked binding of LRP4 to MuSK even at 100 μg IgG (figure 3B).

Passive transfer model exhibits reduced ColQ signals at the NMJs. As described in the introduction, active and passive immunization of model animals reveals reduction of AChRs at the NMJs[24, 26-29], but an effect of MuSK-IgG on ColQ-tailed AChE has not been examined to date. We thus injected IgG of Ct. 2 and Pt. 2 for 14 days to C57BL/6J female mice and visualized AChR, ColQ, MuSK, and AChE in quadriceps muscle sections. Signal intensities of ColQ and AChE were prominently reduced, whereas reductions of AChR and MuSK were moderate (figures 4A and 4B). Quantitative analysis of fluorescence signals revealed that signal areas (figure 4C), intensities (figure 4D), and densities (figure 4E) of ColQ in mice injected with Pt. 2 IgG were reduced to 10%, 9%, 18% of those of Ct. 2 IgG, respectively. On the other hand, signal areas (figure 4C), intensities (figure 4D), and densities (figure 4E) of AChR were reduced to 65%, 55%, and 84% of the control, respectively. Similarly, the same parameters of MuSK were reduced to 40%, 33%, and 78% of the control (figures 4C, 4D, and 4E). Mild to moderate reductions of the areas and intensities of AChR and MuSK are likely to represent reduced sizes of the NMJs, because the densities of AChR and MuSK were only marginally affected. In addition, whereas the number of MuSK per AChR remained essentially the same, the number of ColQ per AChR was reduced to 18% of the control (figure 4F). To summarize, MuSK-IgG compromised anchoring of ColQ-tailed AChE and had a less prominent effect on MuSK and AChR.

Discussion

Molecular bases of MuSK-MG have been examined in cultured cells[30, 31], as well as in active[28, 32] and passive[24, 26, 27] immunization models. Boneva and colleagues report that application of MuSK-MG antibodies to TE671 muscle cells induces inhibition of cell proliferation and secondarily lead to downregulation of AChR and rapsyn[30]. Similarly, Farrugia and colleagues demonstrate that MuSK-MG antibodies have no or minimal effect on the cell surface expression of AChR in TE671 and C2C12 muscle cells[31]. On the other hand,

mice[32] and rabbits[28] immunized with recombinant MuSK develop myasthenic symptoms and NMJ AChR deficiency. Similarly, injection of MuSK-IgG into mice reduces the number of AChRs at the NMJ to 22% of controls, compromises the apposition of the pre- and post-synaptic components of the NMJ[24], and reduces muscle contractility[27]. Cole and colleagues recently report that MuSK-IgG enhances internalization of MuSK from plasma membrane, which leads to progressive dispersal of postsynaptic AChRs by lack of MuSK scaffold and not by disruption of the agrin/LRP4.MuSK signaling pathway[26]. To summarize, MuSK-IgG does not reduce AChR expression in cultured cells, but active and passive immunization of model animals results in AChR deficiency, which is unlikely to be mediated by blocking of the agrin/LRP4/MuSK pathway. Consistent with these findings, our *in vitro* and *in vivo* studies demonstrate that MuSK-IgG blocks an interaction of MuSK and ColQ, and not of MuSK and LRP4. In myotubes of *Colq*-/- mice, the number of membrane-bound MuSK is prominently reduced, and agrin-mediated phosphorylation of the AChR β subunit and the subsequent clustering of AChR are reduced to 30-50% of the wild type[33]. Thus, compromised clustering of AChRs at the NMJs in some MuSK-MG patients could be ascribed to blocking of ColQ binding to MuSK and not to blocking of LRP4 binding to MuSK.

Although our results predict endplate AChE deficiency in MuSK-MG patients, we found no AChE deficiency in intercostal muscles of one reported[34] and two unreported cases of MuSK-MG. *In vitro* microelectrode studies showed a normal EPP decay time constant[35]. In the three MuSK-MG patients observed by us, the MEPC decay times were shorter than normal, normal, and two-fold prolonged[34] compared to controls. Thus, our biopsy findings do not indicate that MuSK-MG patients have endplate AChE deficiency. A plausible explanation for the apparently contradicting observation on the human biopsies and the *in vitro* and *in vivo* studies would be that MuSK-IgGs do not block binding of ColQ-tailed AChE to the NMJ to a detectable extent in the patients. ColQ is localized to the synaptic basal lamina via two mechanisms: one is by binding to heparin sulfate proteoglycans including perlecan[7, 8], and the other is by binding to MuSK[9]. We previously reported that both mechanisms are required for *in vitro* anchoring of human ColQ to the frog NMJ[23]. Reduced clustering of ColQ in our passive transfer model suggests that ColQ needs to bind to at least MuSK in mice. However, binding of ColQ to MuSK is dispensable for clustering ColQ in humans, but is required for facilitating AChR clustering[33].

Ephedrine is effective for congenital endplate AChE deficiency[19, 36] to some extent[37]. Although a high dose of ephedrine blocks AChR channel openings[38, 39], the effectiveness of ephedrine doses used in clinical practice remains unexplained. In a group of MuSK-MG patients who are worsened by cholinesterase inhibitors, anchoring of ColQ-tailed AChE to NMJ may be partly interfered by MuSK IgG and conventional doses of ephedrine may have a beneficial effect.

Acknowledgement

We are grateful to Kenji Otsuka for his technical assistance. The authors thank the patients who participated in this study.

Disclosure

Drs. Kawakami, Ito, Hirayama, Sahashi, Ohkawara, Masuda, Nishida, and Mabuchi have nothing to disclose. Dr. Engel serves as an Associate Editor of Neurology; receives publishing royalties for Myology 3rd ed. (McGraw-Hill, 2004); and has received research support from the NIH and the Muscular Dystrophy. Dr. Ohno has received Grants-in-Aids from the MEXT and the MHLW of Japan.

References

1. Kim N, Stiegler AL, Cameron TO, et al. Lrp4 Is a Receptor for Agrin and Forms a Complex with MuSK. Cell 2008;135:334-342.
2. Zhang B, Luo S, Wang Q, Suzuki T, Xiong WC, Mei L. LRP4 serves as a coreceptor of agrin. Neuron 2008;60:285-297.
3. Dechiara TM, Bowen DC, Valenzuela DM, et al. The receptor tyrosine kinase MuSK is required for neuromuscular junction formation in vivo. Cell 1996;85:501-512.
4. Okada K, Inoue A, Okada M, et al. The muscle protein Dok-7 is essential for neuromuscular synaptogenesis. Science 2006;312:1802-1805.
5. Wu H, Xiong WC, Mei L. To build a synapse: signaling pathways in neuromuscular junction assembly. Development 2010;137:1017-1033.
6. Krejci E, Thomine S, Boschetti N, Legay C, Sketelj J, Massoulié J. The mammalian gene of acetylcholinesterase-associated collagen. J Biol Chem 1997;272:22840-22847.
7. Deprez P, Inestrosa NC, Krejci E. Two different heparin-binding domains in the triple-helical domain of ColQ, the collagen tail subunit of synaptic acetylcholinesterase. J Biol Chem 2003;278:23233-23242.
8. Peng HB, Xie H, Rossi SG, Rotundo RL. Acetylcholinesterase clustering at the neuromuscular junction involves perlecan and dystroglycan. J Cell Biol 1999;145:911-921.
9. Cartaud A, Strochlic L, Guerra M, et al. MuSK is required for anchoring acetylcholinesterase at the neuromuscular junction. J Cell Biol 2004;165:505-515.
10. Farrugia ME, Vincent A. Autoimmune mediated neuromuscular junction defects. Curr Opin Neurol 2010;23:489-495.
11. Farrugia ME, Robson MD, Clover L, et al. MRI and clinical studies of facial and bulbar muscle involvement in MuSK antibody-associated myasthenia gravis. Brain 2006;129:1481-1492.
12. Evoli A, Tonali PA, Padua L, et al. Clinical correlates with anti-MuSK antibodies in generalized seronegative myasthenia gravis. Brain 2003;126:2304-2311.
13. Sanders DB, El-Salem K, Massey JM, McConville J, Vincent A. Clinical aspects of MuSK antibody positive seronegative MG. Neurology 2003;60:1978-1980.
14. Hatanaka Y, Hemmi S, Morgan MB, et al. Nonresponsiveness to anticholinesterase agents in patients with MuSK-antibody-positive MG. Neurology 2005;65:1508-1509.
15. Pasnoor M, Wolfe GI, Nations S, et al. Clinical findings in MuSK-antibody positive myasthenia gravis: a U.S. experience. Muscle Nerve 2010;41:370-374.
16. McConville J, Farrugia ME, Beeson D, et al. Detection and characterization of MuSK antibodies in seronegative myasthenia gravis. Ann Neurol 2004;55:580-584.
17. Shiraishi H, Motomura M, Yoshimura T, et al. Acetylcholine receptors loss and

postsynaptic damage in MuSK antibody-positive myasthenia gravis. Ann Neurol 2005;57:289-293.

18. Niks EH, van Leeuwen Y, Leite MI, et al. Clinical fluctuations in MuSK myasthenia gravis are related to antigen-specific IgG4 instead of IgG1. J Neuroimmunol 2008;195:151-156.
19. Ohno K, Brengman J, Tsujino A, Engel AG. Human endplate acetylcholinesterase deficiency caused by mutations in the collagen-like tail subunit (ColQ) of the asymmetric enzyme. Proc Natl Acad Sci U S A 1998;95:9654-9659.
20. Okada T, Shimazaki K, Nomoto T, et al. Adeno-associated viral vector-mediated gene therapy of ischemia-induced neuronal death. Methods Enzymol 2002;346:378-393.
21. Horejsi J, Smetana R. The isolation of gamma globulin from blood-serum by rivanol. Acta Med Scand 1956;155:65-70.
22. Feng G, Krejci E, Molgo J, Cunningham JM, Massoulie J, Sanes JR. Genetic analysis of collagen Q: roles in acetylcholinesterase and butyrylcholinesterase assembly and in synaptic structure and function. J Cell Biol 1999;144:1349-1360.
23. Kimbell LM, Ohno K, Engel AG, Rotundo RL. C-terminal and heparin-binding domains of collagenic tail subunit are both essential for anchoring acetylcholinesterase at the synapse. J Biol Chem 2004;279:10997-11005.
24. Cole RN, Reddel SW, Gervasio OL, Phillips WD. Anti-MuSK patient antibodies disrupt the mouse neuromuscular junction. Ann Neurol 2008;63:782-789.
25. Toyka KV, Drachman DB, Griffin DE, et al. Myasthenia gravis. Study of humoral immune mechanisms by passive transfer to mice. N Engl J Med 1977;296:125-131.
26. Cole RN, Ghazanfari N, Ngo ST, Gervasio OL, Reddel SW, Phillips WD. Patient autoantibodies deplete postsynaptic muscle-specific kinase leading to disassembly of the ACh receptor scaffold and myasthenia gravis in mice. J Physiol 2010;588:3217-3229.
27. ter Beek WP, Martinez-Martinez P, Losen M, et al. The effect of plasma from muscle-specific tyrosine kinase myasthenia patients on regenerating endplates. Am J Pathol 2009;175:1536-1544.
28. Shigemoto K, Kubo S, Maruyama N, et al. Induction of myasthenia by immunization against muscle-specific kinase. J Clin Invest 2006;116:1016-1024.
29. Jha S, Xu K, Maruta T, et al. Myasthenia gravis induced in mice by immunization with the recombinant extracellular domain of rat muscle-specific kinase (MuSK). J Neuroimmunol 2006;175:107-117.
30. Boneva N, Frenkian-Cuvelier M, Bidault J, Brenner T, Berrih-Aknin S. Major pathogenic effects of anti-MuSK antibodies in myasthenia gravis. J Neuroimmunol 2006;177:119-131.
31. Farrugia ME, Bonifati DM, Clover L, Cossins J, Beeson D, Vincent A. Effect of sera

from AChR-antibody negative myasthenia gravis patients on AChR and MuSK in cell cultures. J Neuroimmunol 2007;185:136-144.

32. Jha S, Xu K, Maruta T, et al. Myasthenia gravis induced in mice by immunization with the recombinant extracellular domain of rat muscle-specific kinase (MuSK). J Neuroimmunol 2006;175:107-117.
33. Sigoillot SM, Bourgeois F, Lambergeon M, Strochlic L, Legay C. ColQ controls postsynaptic differentiation at the neuromuscular junction. J Neurosci 2010;30:13-23.
34. Selcen D, Fukuda T, Shen X-M, Engel AG. Are MuSK antibodies the primary cause of myasthenic symptoms? Neurology 2004;62:1945-1950.
35. Niks EH, Kuks JB, Wokke JH, et al. Pre- and postsynaptic neuromuscular junction abnormalities in musk myasthenia. Muscle Nerve 2010.
36. Ohno K, Engel AG, Brengman JM, et al. The spectrum of mutations causing endplate acetylcholinesterase deficiency. Ann Neurol 2000;47:162-170.
37. Mihaylova V, Muller JS, Vilchez JJ, et al. Clinical and molecular genetic findings in COLQ-mutant congenital myasthenic syndromes. Brain 2008;131:747-759.
38. Sieb JP, Engel AG. Ephedrine: effects on neuromuscular transmission. Brain Res 1993;623:167-171.
39. Milone M, Engel AG. Block of the endplate acetylcholine receptor channel by the sympathomimetic agents ephedrine, pseudoephedrine, and albuterol. Brain Res 1996;740:346-352.

Figure Legends

Figure 1. MuSK-IgG recognizes the NMJ of *Colq*-/- mice.

Non-reducing **(A)** and reducing **(B)** SDS-PAGE of serum proteins and purified IgG of Pt. 1. Gels are stained with Coomassie brilliant blue. M, molecular weight markers; 1, serum before purification; 2, purified IgG. Arrowheads point to IgG of 160 kD **(A)**, as well as the heavy (50 kD) and light (25 kD) chains of IgG **(B)**. **(C)** *In vitro* overlay of purified IgG on a 10-μm skeletal muscle section of *Colq*-/- mice. IgG is visualized with FITC-labeled anti-human IgG and AChR with Alexa594-labeled α-bungarotoxin. Scale bar = 50 μm.

Figure 2. *In vitro* overlay assays.

Purified recombinant ColQ-tailed AChE was overlaid on a 10-μm quadriceps muscle section of *Colq*-/- mice in the presence of the indicated purified MuSK-IgG. ColQ is stained with anti-ColQ antibody and AChR with Alexa594-labeled α-bungarotoxin. Scale bar = 50 μm.

Figure 3. *In vitro* plate-binding assays.

(A) Increasing amounts of MuSK-IgG block binding of the purified recombinant ColQ-tailed AChE to the extracellular domain of human MuSK that is coated on a 96-well plate. Bound ColQ-tailed AChE is quantified by AChE activity. AChE activities are normalized for that at 1 pg IgG of each sample. Mean and SEM of three experiments are plotted. *$p < 0.01$ between controls and patients. **(B)** MuSK-IgG does not block binding of the purified FLAG-tagged extracellular domain of human LRP4 (LRP4N-FLAG) to MuSK that is coated on a 96-well plate. Bound LRP4N-FLAG is quantified with anti-FLAG-HRP. HRP activities are normalized for that at 1 pg IgG of each sample. Mean and SEM of three experiments are plotted.

Figure 4. Passive transfer of MuSK-IgG of Ct. 2 and Pt. 2 to C57BL/6J mice.

(A and B) Quadriceps muscle sections of mice injected IgG of Ct. 2 or Pt. 2 are stained for AChR by Alexa594-labeled α-bungarotoxin, ColQ and MuSK by immunostaining, AChE by cytochemical staining. Scale bar = 40 μm. Signal areas **(C)**, intensities **(D)**, and densities (intensity/area) **(E)** of the indicted molecules per NMJ are shown in mean and SE. **(F)** Densities of ColQ and MuSK are normalized for the density of AChR to estimate the number of ColQ and MuSK per AChR. For AChR, ColQ, and MuSK, we analyzed 44 NMJs of Ct. 2 and 23 NMJs of Pt. 2. For MuSK, we analyzed 82 NMJs of Ct. 2 and 42 NMJs of Pt. 2. Areas and intensities are quantified by the BZ-9000 microscope (Keyence). *$p < 0.05$, ***$p < 0.001$. ns, not significant.

Supplemental Figure 1. Western blot of a newly raised rabbit polyclonal anti-ColQ antibody (1:1000).

Our antibody detects a single 47-kDa fragment of ColQ expressed in nascent HepG2 cells.

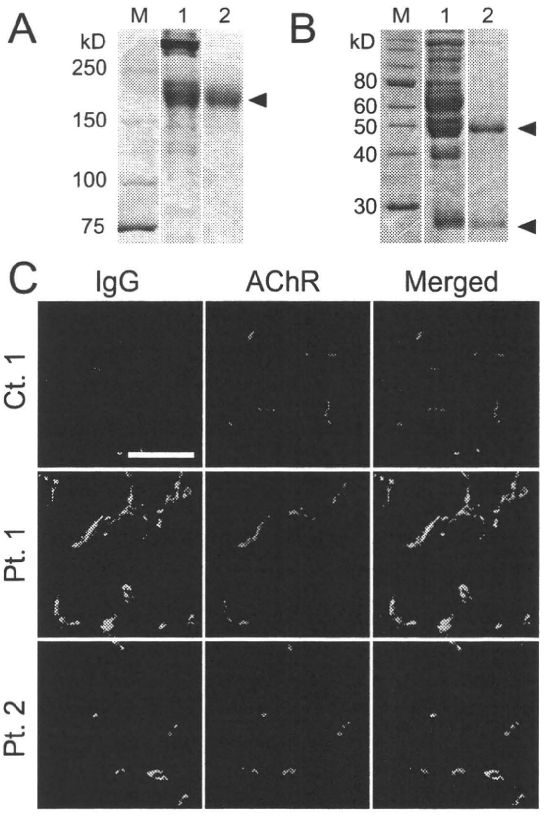
A
M 1 2
kD
250
150
100
75
B
M 1 2
kD
80
60
50
40
30
C
IgG
AChR
Merged
Ct. 1
Pt. 1
Pt. 2

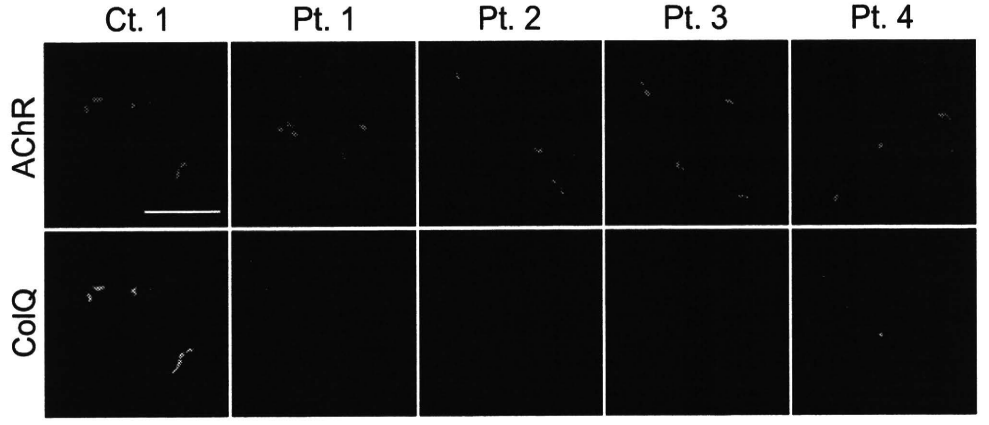
Ct. 1
Pt. 1
Pt. 2
Pt. 3
Pt. 4
AChR
ColQ

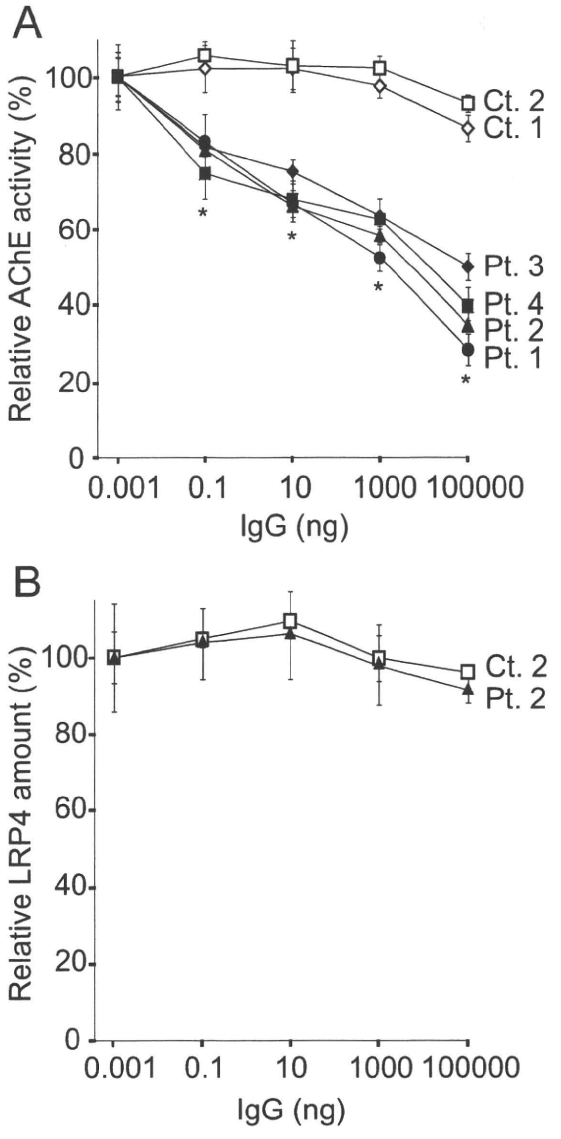
A
Relative AChE activity (%)
100
80
60
40
20
0
0.001
0.1
10
1000
100000
IgG (ng)
Ct. 2
Ct. 1
Pt. 3
Pt. 4
Pt. 2
Pt. 1
*
B
Relative LRP4 amount (%)
100
80
60
40
20
0
0.001
0.1
10
1000
100000
IgG (ng)
Ct. 2
Pt. 2

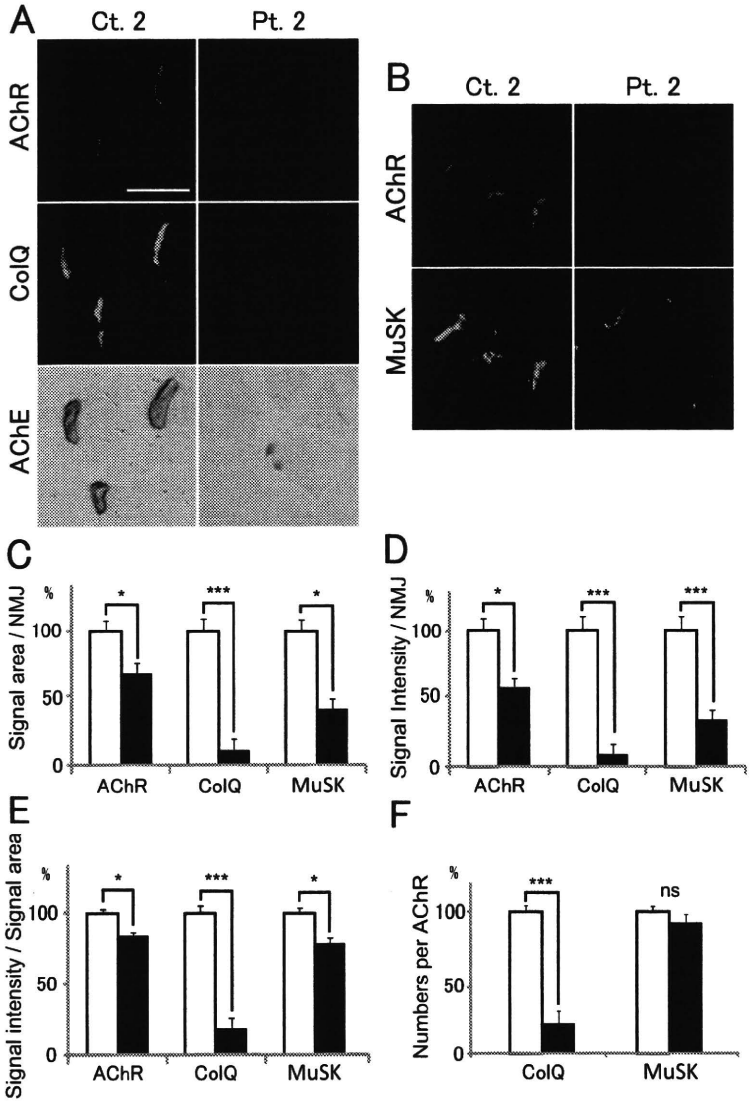
A
Ct. 2
Pt. 2
AChR
ColQ
AChE
B
Ct. 2
Pt. 2
AChR
MuSK
C
Signal area / NMJ
%
100
50
0
*
***
*
AChR
ColQ
MuSK
D
Signal Intensity / NMJ
%
100
50
0
*
***
***
AChR
ColQ
MuSK
E
Signal intensity / Signal area
%
100
50
0
*
***
*
AChR
ColQ
MuSK
F
Numbers per AChR
%
100
50
0
***
ns
ColQ
MuSK

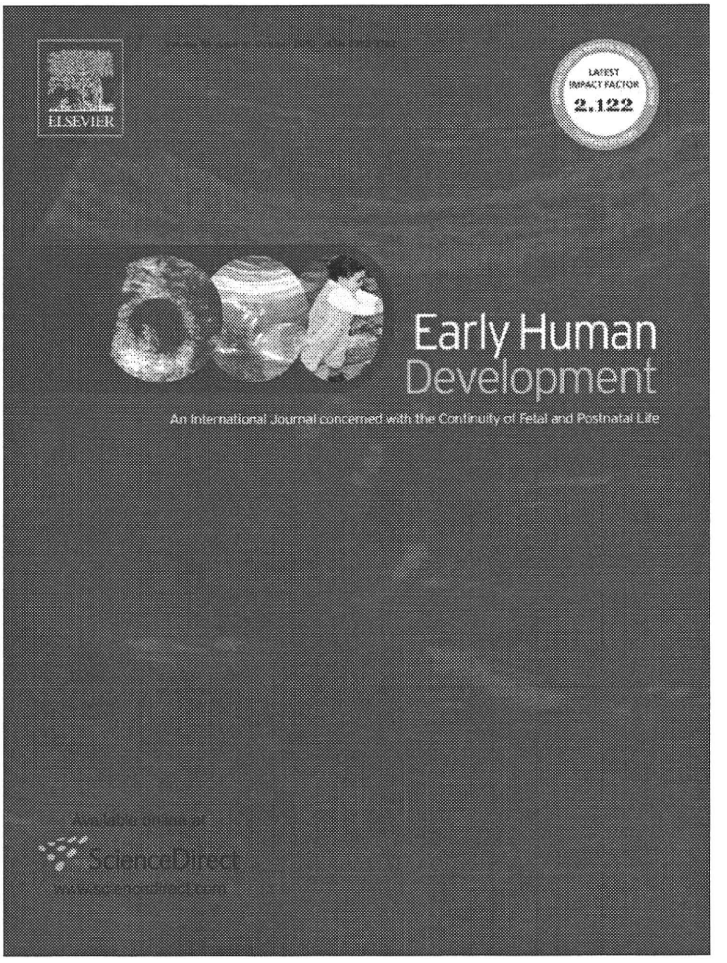

Early Human Development 86 (2010) 665–667

Contents lists available at ScienceDirect

Early Human Development

journal homepage: www.elsevier.com/locate/earlhumdev

Altered gene expression in umbilical cord mononuclear cells in preterm infants with periventricular leukomalacia

Akihisa Okumura [a,*], Toshiyuki Yamamoto [b], Hiroyuki Kidokoro [c], Toru Kato [d], Tetsuo Kubota [c], Hiromichi Shoji [a], Hiroaki Sato [e], Keiko Shimojima [b], Toshiaki Shimizu [a]

[a] Department of Pediatrics, Juntendo University Faculty of Medicine, Japan
[b] International Research and Educational Institute for Integrated Medical Sciences, Tokyo Women's Medical University, Japan
[c] Department of Pediatrics, Anjo Kosei Hospital, Japan
[d] Department of Pediatrics, Okazaki City Hospital, Japan
[e] Department of Pediatrics, Juntendo Shizuoka Hospital, Japan

ARTICLE INFO

Article history:
Received 1 June 2010
Received in revised form 5 September 2010
Accepted 14 September 2010

Keywords:
Periventricular leukomalacia
Ribosomal protein
Gene expression
Preterm infants

ABSTRACT

Aim: Periventricular leukomalacia (PVL) is one of the most important causes of adverse outcome of preterm infants. We hypothesized that inflammatory or some other specific pathways will have been activated at birth in preterm infants who later develop PVL. The aim of this study is to examine the difference in mRNA expression in umbilical cord blood according to the presence or absence of PVL.

Methods: A total of 61 umbilical cord blood samples were collected from preterm infants with gestational age less than 33 weeks together with the patients' medical information during perinatal period. RNA expression patterns in the collected cord bloods were analyzed by microarray. On the basis of cranial ultrasonography and brain MRI examination, 3 infants (4.9%) were diagnosed as cystic PVL and selected as the subjects. Five patients who showed similar perinatal factors to those of infants with PVL but did not show PVL were selected as the normal control.

Results: Five of the 15 up-regulated genes are coding ribosomal proteins, and another encodes a translation elongation factor. Three of the 7 down-regulated genes encode proteins that may be related to immune response and/or inflammation.

Conclusions: Up-regulation of the ribosomal proteins may indicate an activation of lymphocytes during the fetal period.

1. Introduction

Periventricular leukomalacia (PVL) is one of the most important causes of adverse outcome of preterm infants. PVL occurs in approximately 5% of premature infants and is closely related to cerebral palsy and/or cognitive impairment. Although pathogenic mechanisms of PVL have not been fully understood, it is related to two major initiating mechanisms, ischemia and infection/inflammation [1]. Especially, ischemia is widely accepted as a principal upstream initiating mechanism in the pathogenesis of PVL [1]. Recent studies have focused on a pathogenetic role of maternal intrauterine infection and fetal systemic inflammation [2]. The hypothesis is that the fetal systemic inflammatory response leads to white matter injury, perhaps through systemic cytokine release. Although several difficulties with the cytokine hypothesis have been noted [3,4], neuropathologic studies have shown a brisk inflammatory response in white matter mediated by microglia [5,6]. Cytokines amplify the generation of free radicals and changes in glutamate release and uptake that result in enhanced excitotoxicity [7].

Our previous studies revealed that most preterm infants with PVL have acute stage EEG abnormalities since the first few days of life [8,9]. Therefore, we presume that the timing of injury must be ante- or perinatal in most preterm infants with PVL. Antenatal factors should be investigated intensively in order to clarify the pathogenesis of PVL. For this purpose, we examined mRNA expression in the umbilical cord bloods.

2. Methods

2.1. Recruiting the patients' samples

Under the approval by the institutional ethical committee at Juntendo University School of Medicine, umbilical cord blood samples were recruited from preterm infants with gestational age less than 33 weeks born at Juntendo University Hospital, Juntendo Shizuoka

* Corresponding author. Department of Pediatrics, Juntendo University, School of Medicine, 2-1-1 Hongo, Bunkyo-ku, Tokyo 113-8421, Japan. Tel.: +81 3 3813 3111; fax: +81 3 5800 1580.
E-mail address: okumura@juntendo.ac.jp (A. Okumura).

0378-3782/$ – see front matter © 2010 Elsevier Ireland Ltd. All rights reserved.
doi:10.1016/j.earlhumdev.2010.09.001

Hospital, Anjo Kosei Hospital, and Okazaki City Hospital in Japan. Written informed consent was obtained from the parents of the participants. The following perinatal clinical information was collected; i.e. gestational age, birth weight, multiple birth, mode of delivery, threatened premature delivery, premature rupture of membranes, maternal fever, clinical chorioamnionitis, pregnancy-induced hypertension, vaginal hemorrhage, tocolysis, and antenatal steroid.

2.2. Cord blood collection and RNA isolation

More than 1 ml of cord bloods was extracted from each umbilical cord and immediately collected in the tube containing 5 ml of RNA later (Qiagen, Hilden, Germany) to keep blood coagulation and RNA degradation. Within 2 days after collection, the samples were transferred to the laboratory and stored at −80 °C until those were analyzed. Total RNAs were extracted using PAXgene Blood RNA Kit (Qiagen).

2.3. Whole RNA expression analyses by microarray

Whole RNAs extracted from the cord bloods were amplified and labeled by Low RNA Input Linear Amplification Kit (Agilent, Palo Alto, CA, USA) according to the protocol recommended by the manufacture, and hybridized on Whole Human Genome 4×44K microarray (Agilent). The scanned and extracted data were examined by GeneSpring ver. 8 (Agilent) and the genes which showed statistically significant changes ($p<0.05$) were extracted.

3. Results

3.1. The recruited patients

A total of 61 samples were recruited. Among them, 3 infants (4.9%) later developed cystic PVL (Table 1). The diagnosis of PVL was made on the basis of cranial ultrasonography and MRI. In addition, EEG during the first 48 h of life showed marked depression of background activities. Thus, the timing of brain injury was presumed to be antenatal in these 3 infants. The remaining 58 infants had normal ultrasonography and MRI and serial EEG did not show abnormal findings throughout the neonatal period. These infants were included into candidates of the control group. We selected the control patients from the candidates in order to match the perinatal factors with that of the 3 patients with PVL. As a result, 5 infants were chosen as the control (Table 1).

3.2. Gene expression analyses

The genes which showed significant changes, up-regulated and down-regulated, in the cord bloods of the patients who showed PVL later were listed on Tables 2 and 3, respectively.

Table 2
Up-regulated genes.

Gene symbol	Description	p-value	Gene function
RPL23	Ribosomal protein L23	0.011	Structural constituent of ribosome
RPL34	Ribosomal protein L34	0.013	Structural constituent of ribosome
CYBB	Cytochrome b-245, beta polypeptide (chronic granulomatous disease)	0.017	Oxidoreductase activity
EEF1B2	Eukaryotic translation elongation factor 1 beta 2 (*EEF1B2*)	0.021	Translation elongation factor activity
MAL	T-cell differentiation protein (*MAL*)	0.024	Integral to membrane
PAGE5	P antigen family, member 5 (prostate associated)	0.027	Tumor antigens
RPL36A	Ribosomal protein L36a	0.029	Structural constituent of ribosome
CIP29	Cytokine induced protein 29 kDa	0.032	DNA/RNA binding
LGALS3	Lectin, galactoside-binding, soluble, 3	0.036	Sugar binding
PAGE2	P antigen family, member 2 (prostate associated)	0.039	Tumor antigens
RPL11	Ribosomal protein L11	0.040	Structural constituent of ribosome
RPS24	Ribosomal protein S24	0.043	Structural constituent of ribosome
IK	IK cytokine, down-regulator of HLA	0.043	Nucleus
CIITA	Class II, major histocompatibility complex, transactivator	0.043	Transcription regulator activity
ACSL6	Acyl-CoA synthetase long-chain family member 6	0.044	Lipid metabolism

Five of the 15 up-regulated genes (*RPL23*, *RPL34*, *RPL36A*, *RPL11*, and *RPS24*) were ribosomal proteins. *RPL23*, *RPL34*, *RPL36A*, and *RPL11* are components of the 60S subunit, and *RPS24* is a component of the 40S subunit. *EEF1B2* is a guanine nucleotide exchange factor involved in the transfer of aminoacylated tRNAs to the ribosome. Although *MAL*, *CIP29*, *IK*, and *CIITA* may potentially be related to immune response and/or inflammation, their functions have not been fully understood.

Three of the 7 down-regulated genes (*IER5*, *BC070091*, and *CYP4F2*) may be related to immune response and/or inflammation, although their function has not been fully elucidated.

4. Discussion

The strength of our study is that the timing of brain injury was determined by the serial EEG recordings beginning immediately after birth [8,10]. All infants with PVL had EEG abnormalities within 48 h

Table 1
Profiles of the infants.

	GA (weeks)	Birth weight (g)	Delivery	Threatened premature delivery	PROM	Maternal fever	Clinical CAM	PIH	Antenatal hemorrhage	Tocolysis	Antenatal steroid
PVL											
Case 1	29	1416	E-CS	Y	N	N	N	N	N	Ritodrine	N
Case 2	30	1170	S-CS	N	Y	N	N	N	N	Ritodrine	Y
Case 3	32	1810	S-CS	Y	N	N	N	N	N	Ritodrine	N
Control											
Control 1	30	1336	S-CS	Y	N	N	N	N	N	Ritodrine	N
Control 2	32	1860	SVD	Y	Y	N	N	N	N	Ritodrine	N
Control 3	28	740	E-CS	N	N	N	N	Y	N	N	Y
Control 4	28	970	S-CS	Y	Y	N	N	N	N	Ritodrine	Y
Control 5	28	1398	E-CS	Y	Y	N	N	N	N	Ritodrine	N

GA: gestational age, PROM: preterm rupture of membranes, CAM: chorioamnionitis, PIH: pregnancy-induced hypertension, E-CS: emergent caesarean section, S-CS: scheduled caesarean section, SVD: spontaneous vaginal delivery.

Table 3
Down-regulated genes.

Gene symbol	Description	*p*-value	Gene function
IER5	Immediate early response 5	0.007	Immune response
POU3F3	POU domain, class 3, transcription factor 3	0.010	Transcription factor
CEBPA	CCAAT/enhancer binding protein, alpha	0.014	Transcription factor binding
SYNGR4	Synaptogyrin 4	0.019	Integral to membrane
CARD9	Caspase recruitment domain family, member 9	0.030	Inflammation and apoptosis
CYP4F2	Cytochrome P450, family 4, subfamily F, polypeptide 2	0.037	Mediator of inflammation
TNK2	Tyrosine kinase, non-receptor, 2	0.041	Amino acid phosphorylation

after birth. This strongly suggests that antenatal factors will cause PVL in the affected infants [8]. There is no biological information of PVL, especially, at the timing of injuries. Since PVL is a brain injury, it would be the best to analyze cerebrospinal fluids. However, it is very hard to accumulate many cerebrospinal fluid samples from preterm infants. Therefore, the difference of RNA expression in the cord PBMC was analyzed in this study under the hypothesis that it is likely to be related to the later development of PVL [10]. Another strength of our study is the strict selection of the control infants. We considered that the strict selection of the control infants is necessary in order to minimize the confounding factors because many maternal factors will affect the gene expression of the infants. We could match the maternal variables of infants with cPVL and control ones appropriately, although the number of control infants was limited.

The results of our study showed up-regulation of several genes encoding ribosomal proteins. Ribosomes build proteins from the genetic instructions held within messenger RNA and are made from complexes of ribosomal proteins and ribosome RNA. Ribosomes consist of two subunits: large (60S) and small (40S) subunits. 60S subunit is composed of ~49 proteins and 40S subunit of ~33 proteins. Four of the up-regulated genes encode a protein which composes 60S subunit and one of them encoded a protein which composes 40S subunit. In addition, one of the up-regulated genes, *EEF1B2*, encodes an elongation factor which is also a component of ribosomes. Elongation factors facilitate the events of translational elongation. We speculate that the up-regulation of genes related to ribosomes may indicate an enhancement of ribosome function. Peripheral blood mononuclear cells (PBMC) in infants with later development of PVL may have been stimulated by some pathomechanism. This is consistent with a hypothesis that the pathogenesis of PVL will have been initiated during the intrauterine life [8].

Some of the up-regulated genes encode a protein which may potentially be related to immune response and/or inflammation. However, it is unlikely that they play a pivotal role in the immune response and/or inflammation that leads to a later development of PVL. On the basis of many studies on the pathogenesis of PVL, one of the principal initiating pathogenetic factors in PVL is maternal or neonatal infection and fetal or neonatal systemic inflammation [4]. The results of our study did not meet this hypothesis. One possible explanation is that clinical chorioamnionitis was not present in any infants in this study. The role of intrauterine infection/inflammation in the pathogenesis of PVL should be further studied in a cohort of infants of the mothers with chorioamnionitis. Another explanation may be that inflammatory process may have occurred almost exclusively in the brain in our infants with PVL. Inflammation on the brain did not affect RNA expression of PBMC. Since PVL is considered to be multifactorial [11], the contribution of intrauterine infection/inflammation cannot be denied on the basis of our study.

The major limitation of our study is a small number of infants with cPVL. The incidence of cPVL is decreasing according to the improvement of perinatal care [12,13]. In fact, the rate of cPVL was below 5% in our cohort. A larger multicenter study is necessary in order to investigate the pathogenesis of cPVL by this method. At present, milder white matter lesions are considered to be related to the psychomotor developmental delay, especially in extremely low birth weight infants [14–17]. Therefore, it would be the next target for our future study.

In conclusion, we found an up-regulation of genes coding ribosomal proteins in PBMCs in the cord blood of preterm infants with cPVL. This may indicate an activation of lymphocytes during the fetal period, although the triggering mechanism has not been identified. This information may help to understand the pathogenesis of PVL in preterm infants.

Conflict of interest statement

We do not have any financial relationships with pharmaceutical companies, medical equipment manufacturers, biomedical device manufacturers, or any companies with significant involvement in the field of health care. We have no conflict of interest in relation to this manuscript.

Acknowledgments

This work was supported by "High-Tech Research Center" Project for Private Universities: matching fund subsidy from the Ministry of Education, Culture, Sports, Science and Technology, and by the grant from the Ministry of Education, Culture, Sports, Science and Technology (20591306).

References

[1] Volpe, JJ. Neurology of the Newborn. Vol. 5th edition. Elsevier; Philadelphia: 2008.
[2] Dammann O, Leviton A. Inflammatory brain damage in preterm newborns: dry numbers, wet lab, and causal inferences. Early Hum Dev 2004;79:1–15.
[3] Edwards AD, Tan S. Perinatal infections, prematurity and brain injury. Curr Opin Pediatr 2006;18:119–24.
[4] Khwaja O, Volpe JJ. Pathogenesis of cerebral white matter injury of prematurity. Arch Dis Child Fetal Neonatal Ed 2008;93:F153–61.
[5] Haynes RL, Abaud O, Li J, Kinney HC, Volpe JJ, Folkerth RD. Oxidative and nitrative injury in periventricular leukomalacia: a review. Brain Pathol 2005;15:225–33.
[6] Kadhim HJ, Tabarki B, Verellen G, De Prez C, Rona AM, Sebire G. Inflammatory cytokines in the pathogenesis of periventricular leukomalacia. Neurology 2001;56:1278–84.
[7] Matute C, Alberdi E, Domercq M, Sánchez-Gómez MV, Pérez-Samartín A, Rodríguez-Antigüedad A, et al. Excitotoxic damage to white matter. J Anat 2007;210:693–702.
[8] Hayakawa F, Okumura A, Kato T, Kuno K, Watanabe K. Determination of timing of brain injury in preterm infants with periventricular leukomalacia with serial neonatal electroencephalography. Pediatrics 1999;104:1077–81.
[9] Kidokoro H, Okumura A, Hayakawa F, Kato T, Maruyama K, Kubota T, et al. Chronologic changes in neonatal EEG findings in periventricular leukomalacia. Pediatrics 2009;124:e477–84.
[10] Watanabe K, Hayakawa F, Okumura A. Neonatal EEG: a powerful tool in the assessment of brain damage in preterm infants. Brain Dev 1999;21:361–72.
[11] Volpe JJ. Brain injury in premature infants: a complex amalgam of destructive and developmental disturbances. Lancet Neurol 2009;8:110–24.
[12] Zeitlin J, Draper ES, Kollée L, Milligan D, Boerch K, Agostino R, et al. Differences in rates and short-term outcome of live births before 32 weeks of gestation in Europe in 2003: results from the MOSAIC cohort. Pediatrics 2008;121:e936–44.
[13] Himmelmann K, Hagberg G, Beckung E, Hagberg B, Uvebrant P. The changing panorama of cerebral palsy in Sweden: IX. Prevalence and origin in the birth-year period 1995–1998. Acta Paediatr 2005;94:287–94.
[14] Woodward LJ, Anderson PJ, Austin NC, Howard K, Inder TE. Neonatal MRI to predict neurodevelopmental outcomes in preterm infants. N Engl J Med 2006;355:685–94.
[15] Spittle AJ, Boyd RN, Inder TE, Doyle LW. Predicting motor development in very preterm infants at 12 months' corrected age: the role of qualitative magnetic resonance imaging and general movements assessments. Pediatrics 2009;123:512–7.
[16] Dyet LE, Kennea N, Counsell SJ, Maalouf EF, Ajayi-Obe M, Duggan PJ, et al. Natural history of brain lesions in extremely preterm infants studied with serial magnetic resonance imaging from birth and neurodevelopmental assessment. Pediatrics 2006;118:536–48.
[17] Counsell SJ, Edwards AD, Chew AT, Anjari M, Dyet LE, Srinivasan L, et al. Specific relations between neurodevelopmental abilities and white matter microstructure in children born preterm. Brain 2008;131:3201–8.

European Journal of Medical Genetics 53 (2010) 159–161

Contents lists available at ScienceDirect

European Journal of Medical Genetics

journal homepage: http://www.elsevier.com/locate/ejmg

Chromosomal imbalance letter

Phenotypic overlapping of trisomy 12p and Pallister–Killian syndrome

Eisuke Inage [a], Mitsuyoshi Suzuki [a], Kei Minowa [a], Nahoko Akimoto [a], Ken Hisata [a], Hiromichi Shoji [a], Akihisa Okumura [a], Keiko Shimojima [b], Toshiaki Shimizu [a], Toshiyuki Yamamoto [b,*]

[a] Department of Pediatrics, Juntendo University School of Medicine, Tokyo, Japan
[b] International Research and Educational Institute for Integrated Medical Science (IREIIMS), Tokyo Women's Medical University, 8-1 Kawada-cho, Shinjuku-ku, Tokyo 162 8666, Japan

ARTICLE INFO

Article history:
Received 6 December 2009
Accepted 21 February 2010
Available online 26 February 2010

Keywords:
Chromosome 12
Chromosome 14
12p trisomy
Supernumerary marker chromosome
Microarray-based comparative genomic hybridization (array CGH)
Pallister–Killian syndrome

ABSTRACT

Trisomy of 12p is a rare chromosomal abnormality, which sometimes coexists with other chromosomal anomalies. We report on a patient with a supernumerary chromosome involving chromosomes 12 and 14, which was confirmed by array-comparative genomic hybridization (aCGH). He had developmental delay and dysmorphic features overlapped with those of Pallister–Killian syndrome, which is derived from an isodicentric chromosome 12. The microblepharon identified in our patient is a characteristic feature of 12p trisomy. Further patients are needed to establish the phenotypic difference between trisomy 12p and Pallister–Killian syndrome.

1. Method and detection

1.1. Cytogenetics

G-banded chromosomal analysis of the patient's peripheral blood showed a small supernumerary marker chromosome (SMC) of unknown origin with a karyotype of 47,XY,+mar in all examined cells (Supplemental Fig. 1). Multi-color FISH analysis revealed that the SMC was a fusion chromosome derived from the short arm of chromosome 12 (12 pter to 12p12.2) and an unknown chromosomal fragment which was suspected to be of group D (chromosome 13, 14 and 15) or G (chromosome 21 and 22) chromosomal origin because of the satellite structure (data not shown). To confirm the origin of this SMC, further analysis by microarray-based comparative hybridization (aCGH) was performed.

1.2. aCGH

aCGH analysis was performed using the Human Genome CGH Microarray 105A chip (Agilent Technologies, Palo Alto, CA) according to the manufacturer's protocol [5].

1.3. Chromosomal anomaly

On aCGH, the unknown chromosomal fragment of the SMC was revealed to be formed from the two segments of the chromosome 14q. Genomic copy numbers were visualized using CGH Analytics version 3.5 (Agilent Technologies), and the result was as follows; arr 12p13.33p12.3(33,854–17,928,433) × 3,14q11.1q12(18,149,473–27,850,473) × 3,14q21.3q21.3(45,490,109–47,021,431) × 3 (Supplemental Fig. 1).

1.4. Method of confirmation

The result of aCGH was confirmed by fluorescent *in-situ* hybridization (FISH) with BAC clones used as the probes, RP11-359B12 on 12p13.33, RP11-14J7 on 14q11.2, and RP11-321F3 on 14q21.3 [5]. Thus, the final karyotype was 47,XY,+mar (14p13 → 14q12::14q21.3 → 14q21.3::12p12.3 → 12p13.33), ish + der(14)t(12;14)(RP11-359B12+,RP11-14J7+,RP11-321F3+) (Supplemental Fig. 2). The parental karyotypes were not examined because the parents declined our proposal.

2. Clinical description

The boy of 1 year and 8 months of age is the first child of healthy and non-consanguineous parents. Both parents were 32 years old of age, when he was born at 35 weeks gestation via a Cesarean section

* Corresponding author. Tel.: +81 3 3353 8111; fax: +81 3 3352 3088.
E-mail address: yamamoto@imcir.twmu.ac.jp (T. Yamamoto).

1769-7212/$ – see front matter © 2010 Elsevier Masson SAS. All rights reserved.
doi:10.1016/j.ejmg.2010.02.009

due to growth arrest, which had been noted at 29 weeks of gestation. A fetal cleft lip had also been noted at that time. His apgar scores were 8 and 9 at 1 and 5 min, respectively. His birth weight was 1730 g (10–25th centile), length 42.0 cm (<10th centile), and the head circumference 29.6 cm (<10th centile). At birth, the patient was noted to be hypotonic and showed dysmorphic features including a cleft lip and palate, micrognathia, right cryptorchidism, and a rocker-bottom foot deformity. Postnatal head, cardiac, and abdominal ultrasonography revealed no other abnormalities.

After birth, bottle feeding was successful with cleft palate teats. Full enteral nutrition was obtained on day 4. However, inspiratory stridor and retraction gradually developed due to falling back of the tongue, micrognathia and laryngomalacia. Intubation was performed on day 54. After his respiratory status had been stabilized, elective tracheostomy was performed on day 120. His postoperative course was uneventful, and he did not required mechanical ventilation. Palatoplasty was performed on day 202 without surgical complications. Brain magnetic resonance imaging (MRI) showed hypoplasia of the corpus callosum (Fig. 1). Although an electroencephalogram revealed no abnormalities, auditory brainstem response revealed bilateral delay in the 1st wave. Muscular hypotonus persisted after discharge on day 247. His development was delayed with head control at 9 months and rolling over at 12 months. He is presently 1 year and 8 months old and can sit alone but cannot crawl. His growth is below standard with a height of 76.8 cm (<10th centile), a weight of 8605 g (<25th centile), and a head circumference 46.0 cm (<25th centile). He showed dysmorphic facial features including sparse hair and eyebrows, hypertelorism, a wide and depressed nasal bridge, a short nose with wide and anteverted nares, up-slanting palpebral fissures, epicanthic folds, full cheeks, a long philtrum, micrognathia, and a short neck (Fig. 1). His eyes maintained open when he was sleeping, which indicated bilateral microblepharon.

3. Discussion

In the present study, we encountered a patient with an SMC, which was consisted with the short arm of chromosome 12 and two segments of chromosome 14, which were the short arm and the centromeric part of chromosome 14q. According to the report by Liehr et al. patients with SMCs of the centromeric region of chromosome 14 did not show any significant clinical manifestation [2]. Volleth et al. reported a patient with partial trisomy 14pter-q13 and partial monosomy 15pter-q11.2 whose clinical manifestations were mainly derived from partial monosomy 15 [10].

Furthermore, the additional small fragment of 14q21.3 included only two genes, ribosomal protein L10-like (*RPL10LI*) and MAM domain-containing glycosylphosphatidylinositol anchor 2 (*MDGA2*), which encode proteins with unknown function. From these findings, we believe that partial trisomy of chromosome 14 did not have a significant influence on the phenotype and that most of the phenotypic features of this patient are derived from the gain of 12p and are quite similar to those of pure trisomy 12p [4,7].

Partial duplication of 12p is a well-defined entity, characterized by an increased birth weight, hypotonia, macrocephaly, a high forehead, prominent cheeks, a flat face, a large philtrum, a short nose with anteverted nares, a broad everted lower lip, and a short neck. However, pure duplications are rare, and the majority of the reported patients carrying the region for the syndrome seem to be delimited to 12p13.2 pter and 12p13.1p13.3 [3]. Allen et al. presented a patient with der(22)t(12;22)(p10;q10) whose physical findings resembled tetrasomy of 12p [1], and a broad clinical overlap between tetrasomy 12p syndrome and trisomy 12p has been previously suggested [6,11]. Tetrasomy of 12p is often seen as isodicentric chromosome 12p, which is clinically recognized as Pallister–Killian Syndrome (PKS) [9]. Most patients with PKS show tissue-limited mosaicism of isodicentric chromosome 12p, and the characteristic features include severe mental retardation, seizures, hypotonia, and dysmorphic features including a high and prominent forehead, sparse hair and eyebrows, up-slanting palpebral fissures, hypertelorism, epicanthic folds, a wide and depressed nasal bridge, a short nose with anteverted nares, full cheeks, a long philtrum, a short neck, and small and broad hands with short fingers [9,11]. Although the impression of the facial appearance of the present patient is different from that of PKS, there are some overlapping dysmorphic features including the sparse hair and eyebrows, hypertelorism, a wide and depressed nasal bridge, a short nose with wide and anteverted nares, up-slanting palpebral fissures, epicanthic folds, full cheeks, a long philtrum, and a short neck (Table 1). The clear difference from PKS is the microblepharon seen in the present patient, which was also reported in a patient with duplication of 12p [8]. This recurrent occurrence suggests that the microblepharon is a part of the phenotype of trisomy 12p. The other differences were seizures, dysmorphic ears, macroglossia,

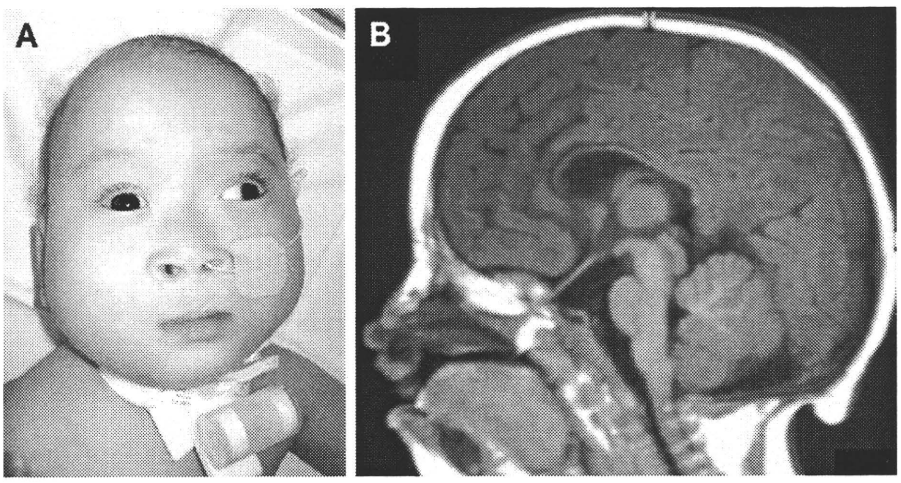

Fig. 1. Clinical information of the patient. A: A picture at the age of 1 years and 8 months. The prominent forehead, sparse hair and eyebrows, hypertelorism, a wide and depressed nasal bridge, a short nose with wide and anteverted nares, up-slanting palpebral fissures, epicanthic folds, full cheeks, a long philtrum, micrognathia, and a short neck can be seen. B: A sagittal image of the brain MRI indicates hypoplasia of the corpus callosum.

Table 1
Clinical features of the presenting patient compared to those of PKS and trisomy 12p.

	PKS	Trisomy 12p	Present patient
Mental retardation	+	+	+
Seizures	+	±	–
Hypotonia	+	+	+
Sparse scalp hair	+	–	+
Prominent forehead	+	+	+
Flat occiput	+	–	–
Hypertelorism	+	+	+
Epicanthus	+	+	+
Microblepharon	–	±	+
Dysmorphic ears	+	+	–
Short nose	+	+	+
Anteverted nostrils	+	+	+
Long philtrum	+	+	+
Macroglossia	+	+	–
Micrognathia	–	±	+
Everted lower lip	+	+	+
Short neck	+	+	+
Accessory nipples	±	±	+
Axillary focal aplasia cutis	+	–	+
Hypo- or hyper-pigmented areas	+	–	+
Short hands and feet	+	+	–

and short hands and feet, which are commonly seen in patients with PKS, but were not identified in the present patient.

Further patients are needed to establish the phenotypic difference between trisomy 12p and PKS.

Conflict of interest

The authors declare no conflict of interest.

Acknowledgments

This work was supported by the International Research and Educational Institute for Integrated Medical Sciences, Tokyo Women's Medical University, which is supported by the Program for Promoting the Establishment of Strategic Research Centers, Special Coordination Funds for Promoting Science and Technology, Ministry of Education, Culture, Sports, Science and Technology (Japan).

Appendix. Supplementary material

Supplementary data associated with this article can be found in the online version at doi:10.1016/j.ejmg.2010.02.009.

References

[1] T.L. Allen, A.R. Brothman, J.C. Carey, P.F. Chance, Cytogenetic and molecular analysis in trisomy 12p. Am. J. Med. Genet. 63 (1996) 250–256.
[2] T. Liehr, K. Mrasek, A. Weise, A. Dufke, L. Rodriguez, et al., Small supernumerary marker chromosomes – progress towards a genotype-phenotype correlation. Cytogenet. Genome Res. 112 (2006) 23–34.
[3] A. Rauch, U. Trautmann, R.A. Pfeiffer, Clinical and molecular cytogenetic observations in three cases of "trisomy 12p syndrome". Am. J. Med. Genet. 63 (1996) 243–249.
[4] R. Segel, I. Peter, L.A. Demmer, J.M. Cowan, J.D. Hoffman, et al., The natural history of trisomy 12p. Am. J. Med. Genet. A 140 (2006) 695–703.
[5] K. Shimojima, T. Inoue, Y. Fujii, K. Ohno, T. Yamamoto, A familial 593-kb microdeletion of 16p11.2 associated with mental retardation and hemivertebrae. Eur. J. Med. Genet. 52 (2009) 433–435.
[6] R. Smigiel, J. Pilch, I. Makowska, H. Busza, R. Slezak, et al., The Pallister–Killian syndrome in a child with rare karyotype – a diagnostic problem. Eur. J. Pediatr. 167 (2008) 1063–1065.
[7] S. Stengel-Rutkowski, A. Albert, J.D. Murken, K. Zahn-Messow, A. Rodewald, et al., New chromosomal dysmorphic syndromes. 4. Trisomy 12p. Eur. J. Pediatr. 136 (1981) 249–262.
[8] M. Tekin, C. Jackson-Cook, A. Pandya, De novo inverted tandem duplication of the short arm of chromosome 12 in a patient with microblepharon. Am. J. Med. Genet. 104 (2001) 42–46.
[9] A. Theisen, J.A. Rosenfeld, S.A. Farrell, C.J. Harris, H.H. Wetzel, et al., aCGH detects partial tetrasomy of 12p in blood from Pallister–Killian syndrome cases without invasive skin biopsy. Am. J. Med. Genet. A 149A (2009) 914–918.
[10] M. Volleth, M. Stumm, J. Burger, P. Muschke, P. Wieacker, Genotype/phenotype correlation in a patient with partial monosomy 15 and partial trisomy 14. Cytogenet. Genome Res. 108 (2005) 283–286.
[11] W. Zumkeller, M. Volleth, P. Muschke, H. Tonnies, A. Heller, et al., Genotype/phenotype analysis in a patient with pure and complete trisomy 12p. Am. J. Med. Genet. A 129A (2004) 261–264.